Excitonic Spin-Coherence Lifetimes in CdSe Nanoplatelets Increase Significantly with Core/Shell Morphology

Phillip I. Martin,^{†1} Shobhana Panuganti,^{†1} Joshua C. Portner,² Nicolas E. Watkins,¹ Mercouri G. Kanatzidis,^{1,3} Dmitri V. Talapin,^{2,4} Richard D. Schaller*^{1,4}

Abstract

We report spin-polarized transient absorption for colloidal CdSe nanoplatelets as functions of thickness (2 to 6 monolayer thickness) and core/shell motif. Using electro-optical modulation of co- and cross-polarization pump-probe combinations, we sensitively observe spin-polarized transitions. Core-only nanoplatelets exhibit few-picosecond spin lifetimes that weakly increase with layer thickness. Spectral content of differenced spin-polarized signals indicate biexciton binding energies that decrease with increasing thickness and smaller values than previously reported. Shell growth of CdS with controlled thicknesses, which partially delocalize the electron from the hole, significantly increases the spin lifetime to ~49 picoseconds at room temperature. Implementation of ZnS shells, which do not alter delocalization but do alter surface termination, increased spin lifetimes up to ~100 ps, bolstering the interpretation that surface termination heavily influences spin coherence, likely due to passivation of dangling bonds. Spin precession in magnetic fields both confirms long coherence lifetime at room temperature and yields excitonic g-factor.

Keywords: 2D semiconductor, CdSe nanoplatelets, spin polarization, transient

Colloidal II-VI semiconductor nanoplatelets (NPLs) constitute attractive candidates for a wide variety of optoelectronics owing to their unique band structure that derives from quantum confinement along a single direction in addition to narrow absorption and emission linewidths that arise from perfect ensemble thickness control with well-defined surface facets. This material class, along with other morphologically similar semiconductors such as two-dimensional (2D) halide perovskites, have garnered interest for their unique spin polarization properties owing to highly controlled material features including tailored thickness of the inorganic semiconductor and, for the II-VI materials, established routes to replace synthetic organic ligands with dielectric inorganic shells. In addition to tuning quantum well thickness, altering particle surface characteristics and controlling electron-hole overlap offer routes to influence spin-depolarization pathways, such as through interaction with surface dangling bonds, which may yield increased spin coherence lifetimes of benefit to spintronics. 11-13

A recent study of colloidal 2D CdSe nanoplatelet quantum wells upon excitation with a circularly polarized pump and cross-polarized probe revealed a short-lived induced absorption at lower-energy wavelengths than the ensemble absorption feature. The red-shifted absorption arises from Coulombic stabilization of biexcitons that show selectivity for the cross-polarized pump-probe combination over the period of time for which pump-induced spin polarization is preserved. Relatedly, co-polarization of circular pump and probe leads to delayed growth of lower-energy

¹Department of Chemistry, Northwestern University, Evanston, IL 60208, USA

²Department of Chemistry, University of Chicago, Chicago, IL 60637, USA

³Materials Science Division and ⁴Center for Nanoscale Materials, Argonne National Laboratory, Lemont, IL 60439, USA

^{*}Corresponding author: schaller@anl.gov, schaller@northwestern.edu

differential induced absorption during the period in which scattering randomizes spin. Such spectral features enable characterization of lifetimes and mechanisms for spin-depolarization of photogenerated excitons that can help to develop understanding regarding fundamentals of exciton dynamics in these materials. 5, 9, 10, 14

In this report, we perform circularly-polarized transient absorption spectroscopy on CdSe NPLs as well as CdSe/CdS and CdSe/ZnS core/shell NPLs in order to discern trends regarding the lifetime of spin-polarization upon increasing particle thickness or shell layer thickness. We observe that as NPL thickness increases from three to six monolayers (MLs) in core-only structures, the spin coherence lifetimes increase proportionally, but fitted lifetimes remain less than 2 ps; the 2ML CdSe NPL sample behaves anomalously, which may relate to appreciably altered lattice properties of this thinnest sample. Circularly polarized TA spectra for these structures convey biexciton binding energies when compared to static absorption, and here are found to be smaller than previously suggested. Spin-polarization lifetimes increase appreciably upon addition of CdS shelllayers to tens of picoseconds. CdS shell growth simultaneously yields surface modification in addition to reduced electron-hole overlap, both of which may increase spin lifetimes. Remarkably, we find that a single ZnS monolayer shell that does not appreciably alter electron-hole overlap also increases spin polarization lifetime significantly, suggesting the key importance of competing surface bonding effects that perhaps dominate electron-hole pair delocalization. Transient Faraday rotation measurements in static magnetic fields further confirm that observed signals arise from spin polarization, and precession frequencies afford exciton g-factor. These findings show that NPL morphology plays an appreciable role in stabilizing exciton spin orientation and can serve to decrease the availability of spin-decay pathways in ways that warrant further examination to achieve technological benefit.

Colloidal NPLs, synthesized according to previously published methods, ^{1-5, 15} were dispersed in hexane for presented optical measurements. Steady-state absorption spectra of the 2.5, 3.5, 4.5, 5.5, and 6.5 ML CdSe NPLs (herein referred to as 2CdSe, 3CdSe, 4CdSe, 5CdSe, 6CdSe, respectively) and CdSe/CdS core/shell NPLs with a 5CdSe core and 1, 3, or 6 ML CdS shell thickness (referred to as 5CdSe/1CdS, 5CdSe/3CdS, 5CdSe/6CdS, respectively) are shown in Figure 1. As the core-only NPL thickness increases, the lowest energy absorption transition redshifts (Figure 1a), while the CdSe/CdS core/shell particles further redshift from the core-only spectrum (for the same 5CdSe NPL core) with increasing shell-layer thickness as quantum confinement and dielectric confinement decrease (Figure 1b).

We performed transient absorption experiments using a 35 fs, amplified titanium:sapphire laser with a 2 kHz repetition rate. Pump pulses produced with an optical parametric amplifier were circularly-polarized using an achromatic zero-order waveplate, maintained at fluences corresponding to ~0.1 excitons per NPL on average, and made coincident on the sample together with mechanically time-delayed, circularly-polarized white light probe pulses. In order to minimize exciton spin-decay via hot carrier relaxation, samples were excited with pump wavelengths near respective absorption onset energies, typically about 10 nm blue of the bandedge transition and with less excess energy than the exciton binding energy (which spans 400 meV for thin cores down to 50 meV for thicker core/shells). Appreciably higher energy photon excitation reduced observed spin-polarized signal amplitudes. Figure 2a shows the experimental configuration and representative transient absorption spectral maps versus pump-probe time-delay measured for the 5CdSe NPL sample. For cross-polarized data (Figure 2b), we observe a photo-induced absorption (PIA) feature near 553 nm that is initially intense and decays within several picoseconds. In the co-polarized TA spectral map (Figure 2c), the PIA is notably weaker initially

but becomes stronger within the first few picoseconds. This low-energy PIA feature is consistent with previous reporting and confers spin-selective excitation of the singly excited, spin polarized exciton to a biexciton state and spin depolarization arising from flipping of either spin in the exciton. 8, 10, 20

To isolate spin-polarized features in the TA maps, transient data was collected using a mechanically chopped pump pulse that was co-polarized with the probe and then subtracted from separately measured cross-polarized data (Figure 2d). Manual subtraction of the independently collected datasets does successfully highlight spectral and temporal features related to spin polarized transitions but is also subject to appreciable noise in quantitative analyses of the exciton dynamics. To improve signal to noise, reduce data acquisition time, and implement a single multichannel detector for the probe pulses, we performed transient absorption measurements by replacing the typical mechanical chopper with an electro-optic inserted into the pump pulse train (see Figure 2a) set to produce half wave rotation at 1 kHz. Co- and cross-polarized pump-probe data were thus collected for immediately sequential pump pulses, not only eliminating the need to routinely collect probe-only spectra, but also decreasing background noise introduced from fluctuations in the pump or probe intensity over experimental lab time. Using this approach, we were able to directly generate polarization-differential transient spectral maps of the spin-dependent photophysical behaviors, as shown in Figure 2e.

Figure 3a shows the dynamic behavior of the spin-selective biexcitonic PIA across CdSe core-only samples as a function of increasing NPL thickness. These kinetic traces were then fit to single exponential decays to evaluate spin coherence lifetimes (Table S1). Over the range of increasing NPL thickness from 3CdSe to 6CdSe, spin-polarized decay lifetime increases from just $0.24~(\pm 0.01)$ ps for 3CdSe up to 1.76 (± 0.12) ps for 6CdSe, as shown in Figure 3b (data plotted to longer time-delays appears as Figure S1). A conceivable origin of this trend may be the reduced prominence of surface atoms as NPL thickness increases that present surface spins which cause depolarization. Notably, the 2CdSe does not fit the otherwise systematic trend, instead exhibiting similar dynamic behavior as 5CdSe, suggesting that other contributing factors in the generation of long-lived spin-polarized species impact the particularly thin 2CdSe NPLs. Thinner NPLs, and especially 2CdSe experiences appreciable strain in comparison to thicker NPLs that feature more internal bonding, which conceivably could disrupt the otherwise systematic trend. ²¹⁻²³ At the same time, the >3 eV energy gap of 2CdSe may play a role if exciton wavefunctions begin to permeate the high potential barrier of the organic surface.²² This thickness dependence for core-only samples conveys lifetimes that are short and comparable to those recently reported for 2D perovskite spin-polarized lifetimes versus inorganic layer thickness. Xiang et. al. reported fast, sub-picosecond decay components as evidence of hole spin-flips in CdSe with longer-lived spin polarization arising from particles that lack rapid hole trapping, 10 but relied on examining differences in dynamics for other exciton transitions that we did not observe. Notably, hole trapping has been implicated to occur on similar timescales as our observations²⁴ and could deleteriously affect excitonic spin polarization.

In addition to spin coherence decay lifetime, differential spin-polarized transient *spectral* maps show clear changes between the lower-energy PIA in comparison to the heavy hole static absorption feature as a function of thickness, with a shift from the static peak that relates biexciton binding energy and an increased linewidth possibly arising from relative spatial position of the second electron hole pair created by the probe²⁰ (see Figure 3c). We find that attractive biexciton binding energy reaches ~50 meV in the 2CdSe core-only NPLs and decreases to ~15 meV in the 6CdSe core-only NPLs (Figure 3d). Reduction of biexciton binding energy is expected as particle

thickness increases and trends in the direction of bulk-like behavior.²⁵ Such biexciton binding energies for 4CdSe have been estimated at up to 45 meV in the literature,⁸ based in part on observation of biexciton-derived gain and lasing redshifts. However, we note that amplified spontaneous emission appears at energies prescribed by optical gain but is also influenced by optical loss from reabsorption. Measurements of binding energy reported in this report suffer less from the latter-described influence and relate a smaller value that is consistent both with other experimental data for 4CdSe^{26, 27} and theory,²⁵ further highlighting the role of reabsorption from small Stokes shifts in gain and lasing efforts.

Figure 4 shows the spin-polarized dynamic behavior of CdSe/CdS core/shell NPL samples that were synthesized using the same 5CdSe core. Spin polarization lifetimes increase significantly for these core/shell structures. Decay kinetics are well-described by biexponential fitting with lifetimes τ_1 and τ_2 (see Fig. S2) for each sample exhibiting a rapid, ~ 1 ps process and a longerlived, up to ~49 ps lifetime (see also Table S2). This longer decay component indicates a significant extension of spin-polarized exciton lifetime relative to the core-only samples. The τ_2 lifetime increases sub-linearly with CdS shell thickness, which suggests diminishing influence on the preservation of spin polarization with both increased total volume of the nanostructure and increased average distance to the organic interface. Quantum confinement, it should be noted, also changes sub-linearly with shell layer thickness. Increases of the exciton spin coherence lifetime clearly arise from features of the core/shell morphology, but a challenge to mechanistic interpretation is that the core/shell system differs in multiple ways from the core-only particles. The core/shell samples experience reduced electron-hole wavefunction overlap for this combination of materials and reduced quantum and dielectric confinement in addition to altered CdSe interface chemistry. The quasi-type-II energy level alignment of the CdSe/CdS conduction bands permits electron delocalization into the CdS shell layer whereas holes nominally remain within the CdSe core. 13 Such delocalization could serve to reduce exchange interaction of the electron with the hole that can facilitate spin relaxation.²⁸ At the same time, isolated spins of dangling bonds and charges at the inorganic-organic interface may offer fast, efficient spin relaxation, 9, 29, 30 but the nearly-matched lattices at the inorganic-inorganic interface can largely reduce the importance of such relaxation processes.

To evaluate influences on CdSe/CdS core/shell spin lifetimes, we also prepared 5CdSe/ZnS core/shell NPLs with 1 or 3 ZnS monolayers. These structures, for which shells were carefully grown via colloidal atomic layer deposition using a fixed 5CdSe core, 5, 15 lack appreciable delocalization of either charge-carrier into this wider gap shell as noted by the absorption spectra shown in Figure 5a. ZnS shell growth does appreciably alter the surface bonding in comparison to organic ligand surface termination. Interestingly, the 5CdSe/1ZnS core/shell sample presented markedly slower spin depolarization relative to the core-only sample as shown in Figure 5b, with a significant amplitude ~100 ps lifetime as well as additional still longer-lived low-amplitude components (see Fig. S3 for biexponential fits and Table S3 for fit parameters). Upon continuing growth to a 3ZnS monolayer shell, lifetime decreases to ~21 ps perhaps influenced as strain builds up with the thicker, small-lattice-spacing shell. Overall, the significant lifetime increase suggests that removal of the proximal organic surface termination or passivation of dangling surface bonds for the core/shell structure serves to increase spin lifetimes in both the CdSe/CdS and CdSe/ZnS systems, consistent with theoretical investigations of Rodina et al.^{21,22} Additionally, this finding suggests that the hole spin relaxation mechanism is not centrally important, as this charge remains contained within the CdSe core for the latter core/shell.

Finally, we performed transient Faraday rotation measurements in different magnetic fields³¹ for the 5CdSe/1ZnS sample. Magnetic field causes the spin polarization to oscillate with the Larmor precession frequency associated with $E=g\mu_BB$. In these experiments field-induced oscillations occur and we find the oscillation frequency scales linearly with magnetic field strength with y-intercept near zero (~230 MHz). By fitting the period of oscillation versus field we obtain an excitonic g-factor of 1.83 that relates contributions of the electron and hole. This value is similar to other reports of exciton g-factor as studied using pump-orientation-probe measurements, such as in work by Feng *et. al.*,³² and further confirms that the long lifetime observed indeed conveys spin coherence.

The spin-depolarization of these states can occur through various mechanisms, including hot carrier relaxation and inelastic collisions with the nanoplatelet surface, that result in rapid spinpolarization decay. There are several common spin-depolarization mechanisms in semiconductors.^{6, 9, 13} In the Elliot-Yafet (EY) mechanism, spin-depolarization occurs through momentum scattering while the Bir-Aronov-Pikus (BAP) mechanism becomes operative in materials where hole concentration is high and exchange scattering with electrons is possible. The relevance of these mechanisms in bulk materials is often dictated by the availability of phonon coupling (in the case of EY) and exchange scattering (in the case of BAP) pathways as affected by temperature, carrier mobilities, and morphology. However, quantum confinement of nanoparticles can result in local structure-induced magnetic fields, such as at the surface, 9, 29, 30 which boosts the dominance of Dyakonov-Perel (DP) pathways that are enabled in structures without inversion symmetry and supported by extended electronic states. Synthetic manipulation of the particle morphology, such as increasing the nanoplatelet thickness or replacing an organic ligand with a more perfectly matched shell layer, alters characteristics of the particle surface, in some cases reducing electron-hole overlap for CdSe/CdS, but in the case of CdSe/ZnS chiefly moves spins of organic ligand termination further from the spin-polarized exciton and reduces the rate of dominant spin-depolarization pathways. Increasing ZnS shell thickness likely increases strain and may introduce cracks in the shell, altering the energy landscape, though this requires more investigation.

Regarding observation of biexponential decays of spin-polarized lifetime, we expect that such observations point to different electronic scenarios for sub-populations within the ensemble with an origin that remains to be investigated. Notably, spin-polarization data for the 5CdSe coreonly sample shown in Fig. 4a does not match that of a different 5CdSe sample shown in Fig. 5b. The former shows a few percent amplitude of a longer-lived spin-polarization that is absent in the latter sample. The observation for the former offers a prospect of long-lived spin polarization in core-only samples if the features of this sub-population might be understood and controlled.

Spin-polarization of excitons created with circularly-polarized laser pulses in core-only CdSe NPLs decay rapidly, occurring on picosecond timescales. Variation in sample morphology, such as particle thickness and surface passivation, are shown to impact and increase spin-depolarization lifetimes, with an increase from $\tau = 0.24$ ps in 3CdSe NPLs to $\tau = 1.76$ ps in 6CdSe NPLs. Growth of CdS shells yielded significant increases in spin-depolarization times, with an order of magnitude effect for thin-shelled samples of 5CdSe/1CdS NPLs ($\tau_2 = 24$ ps) up to $\tau_2 = 48.6$ ps for 5CdSe/6CdS NPLs. Additional measurements conducted on 5CdSe/ZnS samples, which do not alter electron-hole overlap would suggest a key role that surface passivation plays in maintaining excitonic spin coherence. In particular 5CdSe/1ZnS core/shell samples exhibited 100 ps lifetime, which is nearly two orders of magnitude longer than those observed in core-only samples. Studying these effects provides an important step towards understanding how to generate

and maintain long-lived spin-polarized excitonic states in 2D semiconductors. Understanding specific spin-depolarization lifetimes and mechanisms will be valuable for the implementation of these states and materials in future technologies.

Supporting Information

The following information is available free of charge. Nanoplatelet synthesis, spectroscopic methods, and supplementary spin lifetime data.

Acknowledgements

Work performed at the Center for Nanoscale Materials, a U.S. Department of Energy Office of Science User Facility, was supported by the U.S. DOE, Office of Basic Energy Sciences, under Contract No. DE-AC02-06CH11357. We acknowledge student support provided by the National Science Foundation MSN under Grant No. 1808590. S.P. gratefully acknowledges financial support from the National Science Foundation Graduate Research Fellowship Program under Grant No. DGE-1842165 and the Ryan Fellowship. This work was supported in part by the National Science Foundation under Grant No. DMR-2019444 (IMOD an NSF-STC). JP and DVT acknowledge support by the National Science Foundation under Grant No. DMR-2019444 and by MICCoM, as part of the Computational Materials Sciences Program funded by the US Department of Energy, Office of Science, BES, Materials Sciences and Engineering Division under Award 5J-30161-0010A.

Author Contributions

[†]These authors contributed equally to this work

Notes

The authors declare no competing financial interest.

Figures

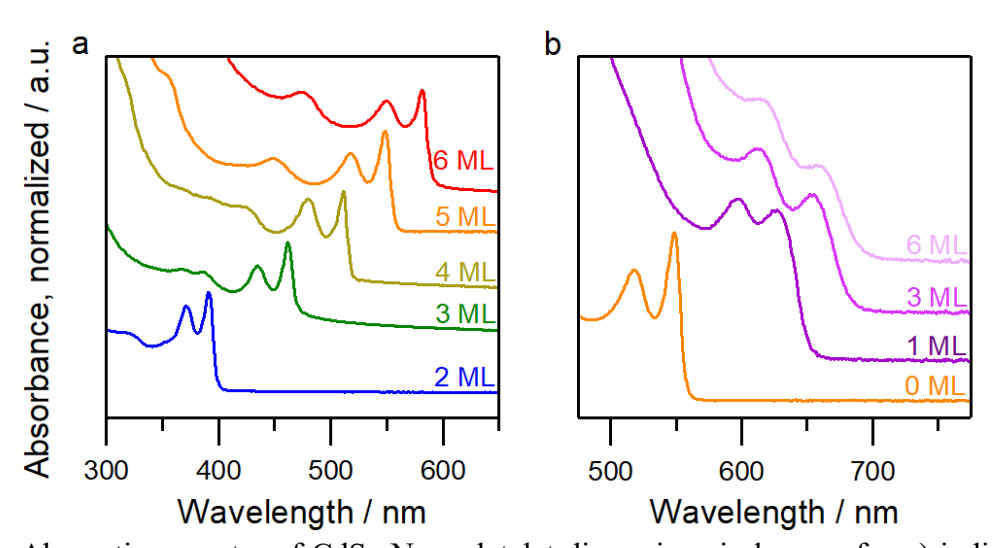


Figure 1. Absorption spectra of CdSe Nanoplatelet dispersions in hexane for **a**) indicated coreonly monolayer thicknesses and for **b**) a 5CdSe NPL core onto which CdS shells of indicated layer thicknesses.

а

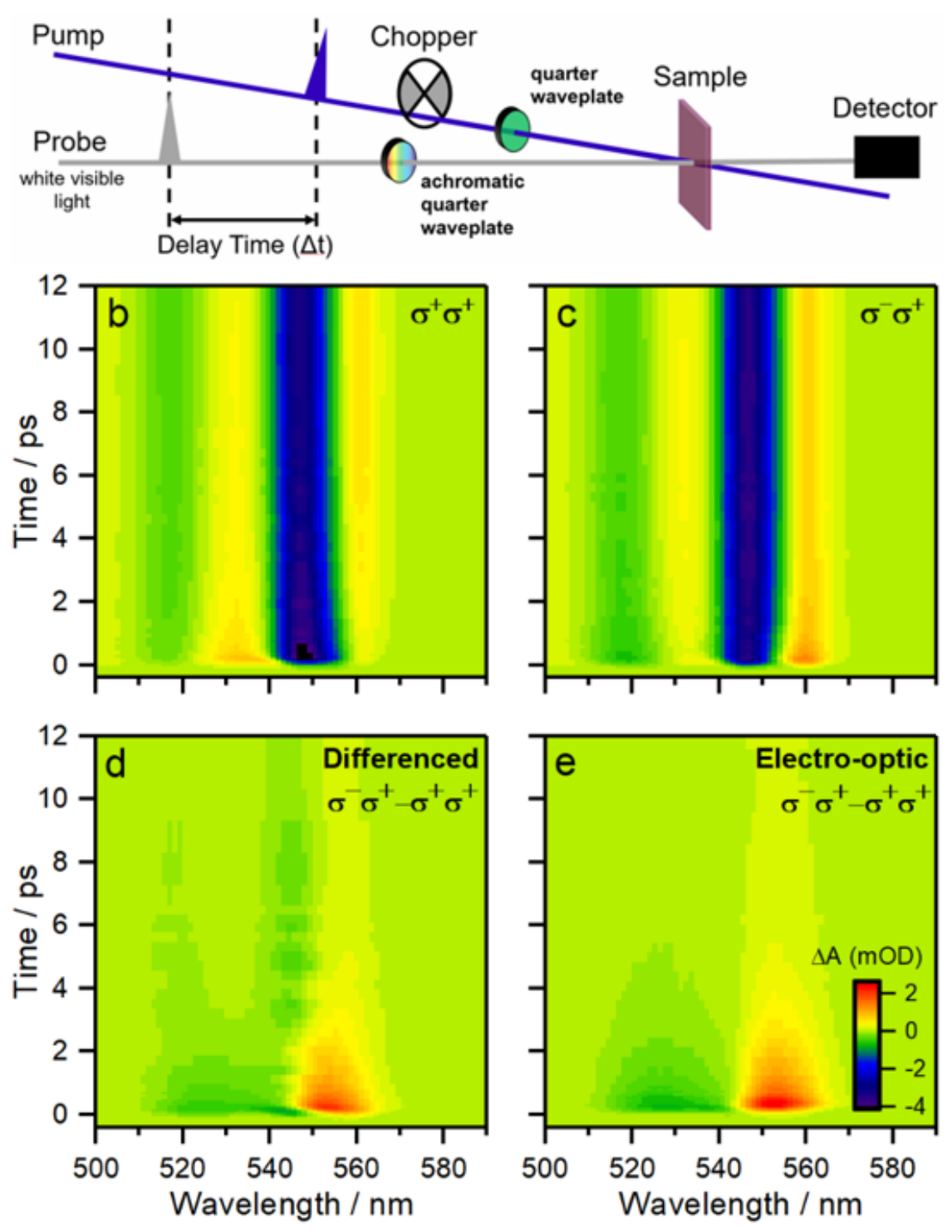


Figure 2. a) Schematic of circularly polarized transient absorption experiments. b, c) Transient absorption spectral maps for indicated pump and probe circular polarization conditions. d) Differencing panel b from panel c highlights time-dependent response of the polarization-dependent spectral information. e) Replacement of the mechanical chopper with an electro-optical modulator directly yielded differential responses of the sample to co-polarized vs cross-polarized pump-probe conditions with increased signal to noise.

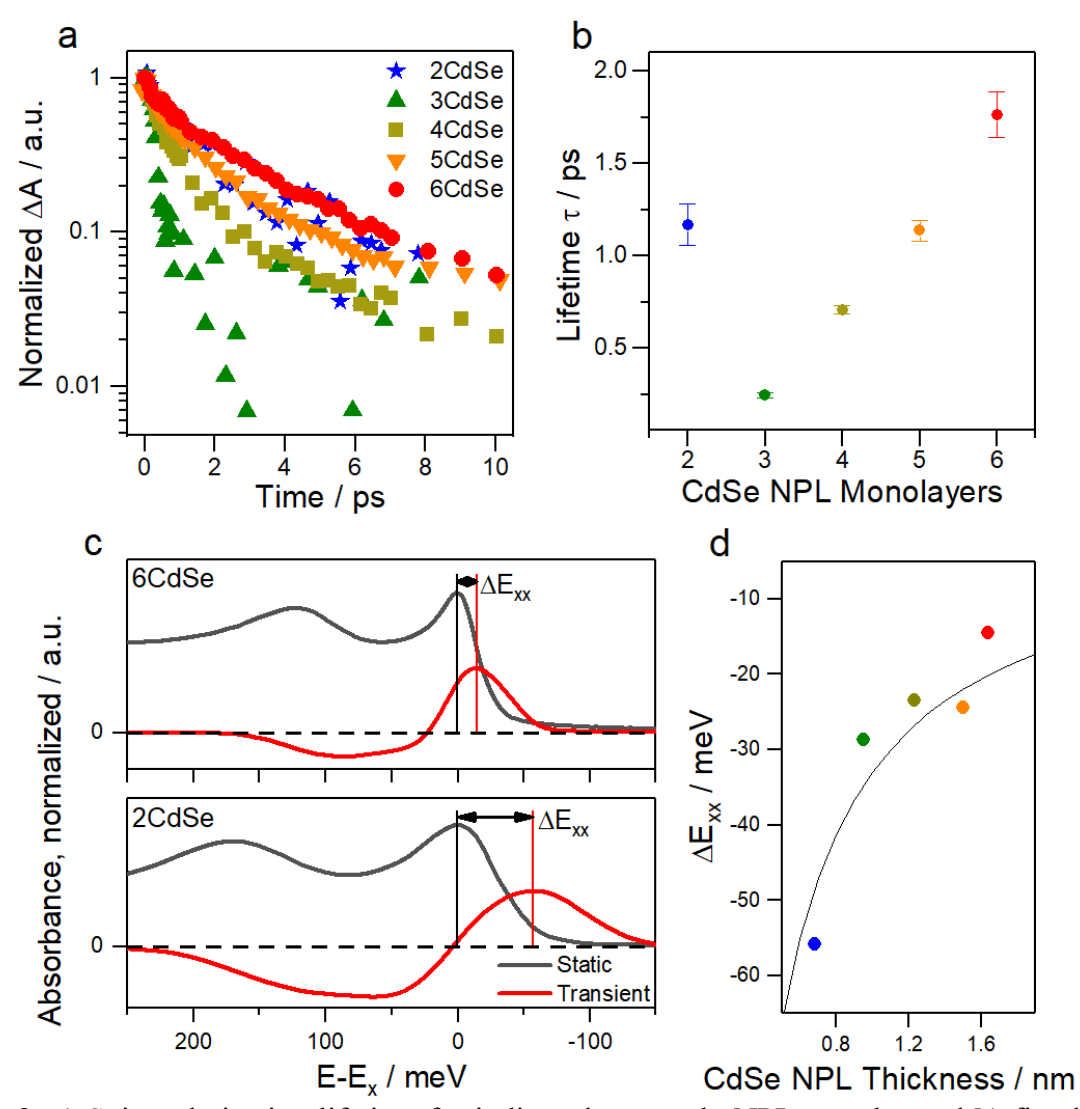


Figure 3. a) Spin polarization lifetime for indicated core-only NPL samples and **b)** fitted decay time constants. **c)** Biexciton binding energy, ΔE_{xx} , evaluated from the spectral shift of the static absorption maximum to that of the transient spin polarized signal. **d)** Biexciton binding energy evaluated for indicated core-only NPL thicknesses spanning 2CdSe to 6CdSe.

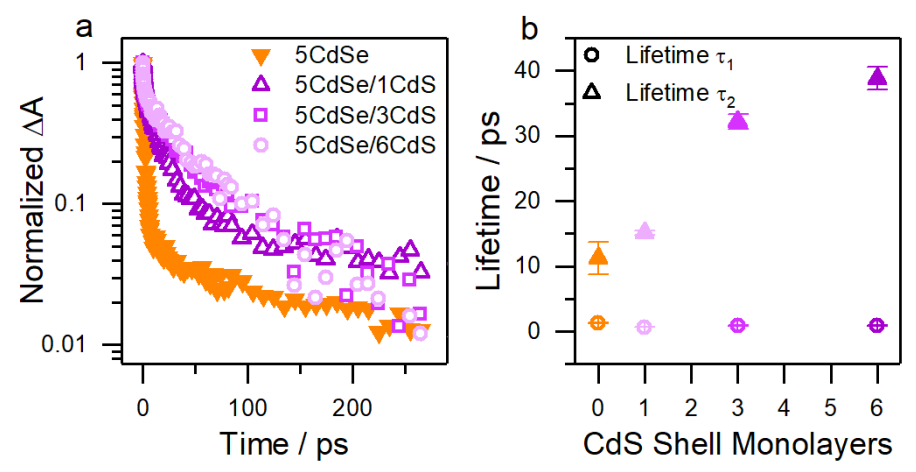


Figure 4. a) Dynamics of CdSe/CdS core/shell NPL samples that were synthesized using the same 5CdSe core. Spin polarization lifetimes increase significantly for these core/shell structures. **b)** Spin polarized decay kinetics are well-described by biexponential fitting with lifetimes τ_1 and τ_2 .

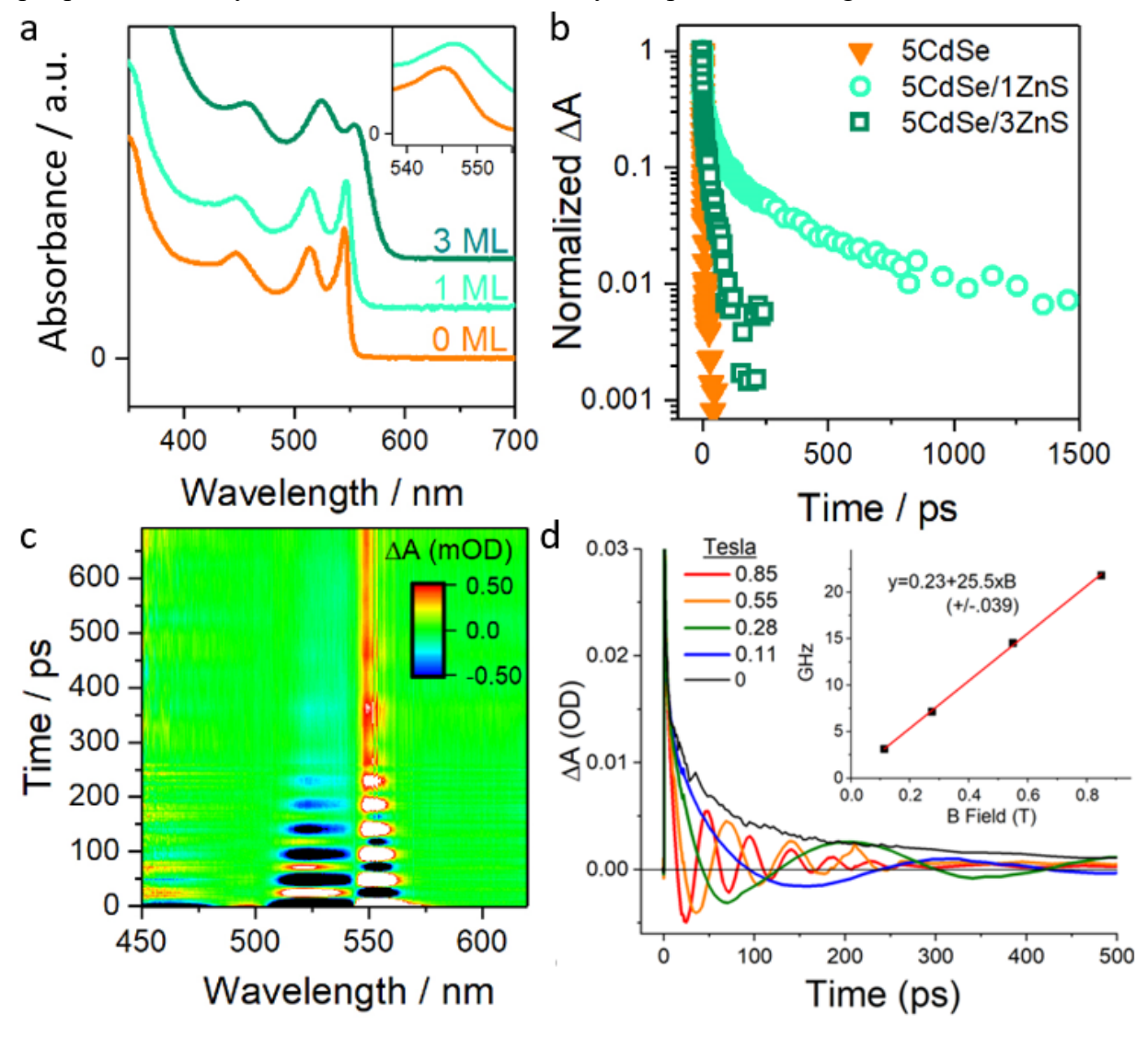


Figure 5. a) Absorption spectra of core/shell NPLs with a 5CdSe core and either 1 or 3 ZnS shell layers. **b)** Pump-polarization-modulated transient response of the three samples in panel A show an appreciable increase in spin polarized lifetime with even 1 layer of ZnS shell growth. **c)** Transient Faraday rotation of a 5CdSe/1ZnS nanoplatelet sample at room temperature shows oscillatory behavior with one discernible frequency. **d)** For the 5CdSe/1ZnS sample, measurement at several different indicated magnetic field strengths (here plotted at 554 nm probe wavelength) shows a linear dependence of oscillation frequency (inset), a g-factor of 1.83, and small y-axis intercept (230 MHz).

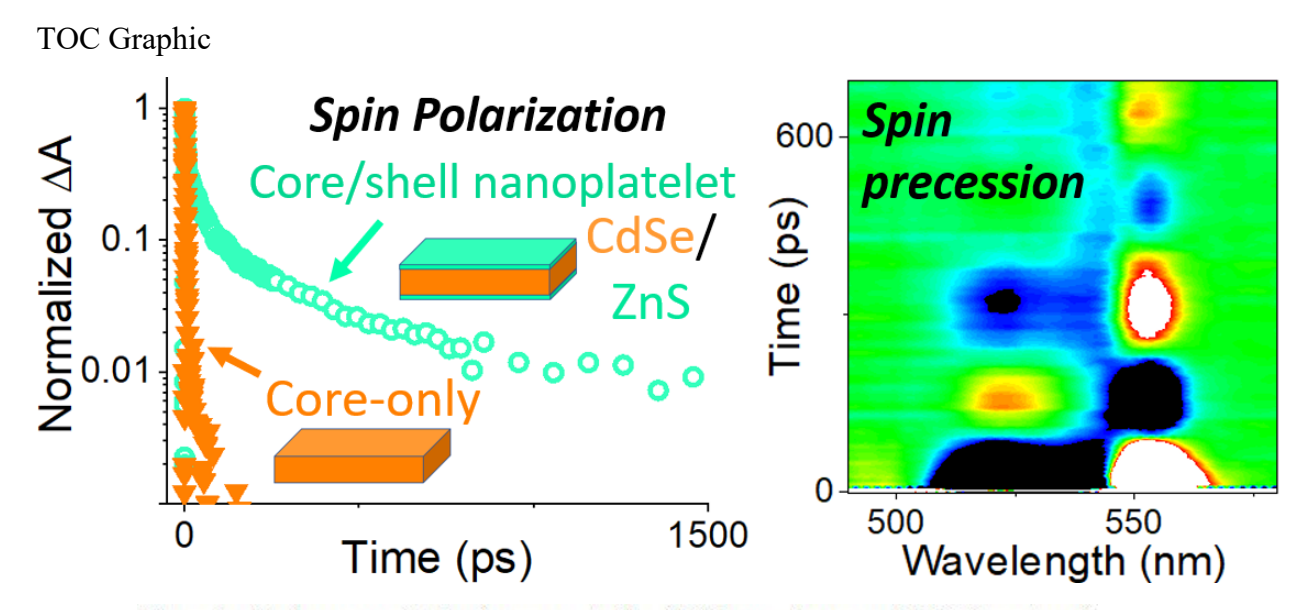
References

- (1) Ithurria, S.; Dubertret, B. Quasi 2D colloidal CdSe platelets with thicknesses controlled at the atomic level. *Journal of the American Chemical Society* **2008**, *130* (49), 16504-16505.
- (2) Ithurria, S.; Tessier, M.; Mahler, B.; Lobo, R.; Dubertret, B.; Efros, A. L. Colloidal nanoplatelets with two-dimensional electronic structure. *Nature Materials* **2011**, *10* (12), 936-941.
- (3) Mahler, B.; Nadal, B.; Bouet, C.; Patriarche, G.; Dubertret, B. Core/shell colloidal semiconductor nanoplatelets. *Journal of the American Chemical Society* **2012**, *134* (45), 18591-18598.
- (4) She, C.; Fedin, I.; Dolzhnikov, D. S.; Dahlberg, P. D.; Engel, G. S.; Schaller, R. D.; Talapin, D. V. Red, yellow, green, and blue amplified spontaneous emission and lasing using colloidal CdSe nanoplatelets. *ACS Nano* **2015**, *9* (10), 9475-9485.
- (5) Hazarika, A.; Fedin, I.; Hong, L.; Guo, J.; Srivastava, V.; Cho, W.; Coropceanu, I.; Portner, J.; Diroll, B. T.; Philbin, J. P. Colloidal atomic layer deposition with stationary reactant phases enables precise synthesis of "digital" II–VI nano-heterostructures with exquisite control of confinement and strain. *Journal of the American Chemical Society* **2019**, *141* (34), 13487-13496.
- (6) Odenthal, P.; Talmadge, W.; Gundlach, N.; Wang, R.; Zhang, C.; Sun, D.; Yu, Z.-G.; Valy Vardeny, Z.; Li, Y. S. Spin-polarized exciton quantum beating in hybrid organic—inorganic perovskites. *Nature Physics* **2017**, *13* (9), 894-899.
- (7) Chen, X.; Lu, H.; Li, Z.; Zhai, Y.; Ndione, P. F.; Berry, J. J.; Zhu, K.; Yang, Y.; Beard, M. C. Impact of layer thickness on the charge carrier and spin coherence lifetime in two-dimensional layered perovskite single crystals. *ACS Energy Letters* **2018**, *3* (9), 2273-2279.
- (8) Geiregat, P.; Tomar, R.; Chen, K.; Singh, S.; Hodgkiss, J. M.; Hens, Z. Thermodynamic equilibrium between excitons and excitonic molecules dictates optical gain in colloidal cdse quantum wells. *The Journal of Physical Chemistry Letters* **2019**, *10* (13), 3637-3644.
- (9) Shornikova, E. V.; Golovatenko, A. A.; Yakovlev, D. R.; Rodina, A. V.; Biadala, L.; Qiang, G.; Kuntzmann, A.; Nasilowski, M.; Dubertret, B.; Polovitsyn, A. Surface spin magnetism controls the polarized exciton emission from CdSe nanoplatelets. *Nature Nanotechnology* **2020**, *15* (4), 277-282.
- (10) Xiang, D.; Li, Y.; Wang, L.; Ding, T.; Wang, J.; Wu, K. Electron and hole spin relaxation in CdSe colloidal nanoplatelets. *The Journal of Physical Chemistry Letters* **2020**, *12* (1), 86-93.
- (11) Kikkawa, J.; Gupta, J.; Malajovich, I.; Awschalom, D. Spin coherence in semiconductors: storage, transport and reduced dimensionality. *Physica E: Low-dimensional Systems and Nanostructures* **2001**, *9* (1), 194-201.
- (12) Ouyang, M.; Awschalom, D. D. Coherent spin transfer between molecularly bridged quantum dots. *Science* **2003**, *301* (5636), 1074-1078.
- (13) Žutić, I.; Fabian, J.; Sarma, S. D. Spintronics: Fundamentals and applications. *Reviews of Modern Physics* **2004**, *76* (2), 323.

- (14) Chen, X.; Lu, H.; Wang, K.; Zhai, Y.; Lunin, V.; Sercel, P. C.; Beard, M. C. Tuning Spin-Polarized Lifetime in Two-Dimensional Metal—Halide Perovskite through Exciton Binding Energy. *Journal of the American Chemical Society* **2021**, *143* (46), 19438-19445.
- (15) Ithurria, S.; Talapin, D. V. Colloidal Atomic Layer Deposition (c-ALD) using Self-Limiting Reactions at Nanocrystal Surface Coupled to Phase Transfer between Polar and Nonpolar Media. *Journal of the American Chemical Society* **2012**, *134* (45), 18585-18590. DOI: 10.1021/ja308088d.
- (16) Benchamekh, R.; Gippius, N. A.; Even, J.; Nestoklon, M.; Jancu, J.-M.; Ithurria, S.; Dubertret, B.; Efros, A. L.; Voisin, P. Tight-binding calculations of image-charge effects in colloidal nanoscale platelets of CdSe. *Physical Review B* **2014**, *89* (3), 035307.
- (17) Brumberg, A.; Harvey, S. M.; Philbin, J. P.; Diroll, B. T.; Lee, B.; Crooker, S. A.; Wasielewski, M. R.; Rabani, E.; Schaller, R. D. Determination of the in-plane exciton radius in 2D CdSe nanoplatelets via magneto-optical spectroscopy. *ACS nano* **2019**, *13* (8), 8589-8596.
- (18) Ji, B.; Rabani, E.; Efros, A. L.; Vaxenburg, R.; Ashkenazi, O.; Azulay, D.; Banin, U.; Millo, O. Dielectric confinement and excitonic effects in two-dimensional nanoplatelets. *ACS nano* **2020**, *14* (7), 8257-8265.
- (19) Shornikova, E. V.; Yakovlev, D. R.; Gippius, N. A.; Qiang, G.; Dubertret, B.; Khan, A. H.; Di Giacomo, A.; Moreels, I.; Bayer, M. Exciton Binding Energy in CdSe Nanoplatelets Measured by One-and Two-Photon Absorption. *Nano letters* **2021**, *21* (24), 10525-10531.
- (20) Rodà, C.; Geiregat, P.; Di Giacomo, A.; Moreels, I.; Hens, Z. Area-Independence of the Biexciton Oscillator Strength in CdSe Colloidal Nanoplatelets. *Nano Letters* **2022**, *22* (23), 9537-9543.
- (21) Delikanli, S.; Yu, G.; Yeltik, A.; Bose, S.; Erdem, T.; Yu, J.; Erdem, O.; Sharma, M.; Sharma, V. K.; Quliyeva, U. Ultrathin highly luminescent two-monolayer colloidal CdSe nanoplatelets. *Advanced Functional Materials* **2019**, *29* (35), 1901028.
- (22) Greenwood, A. R.; Mazzotti, S.; Norris, D. J.; Galli, G. Determining the Structure—Property Relationships of Quasi-Two-Dimensional Semiconductor Nanoplatelets. *The Journal of Physical Chemistry C* **2021**, *125* (8), 4820-4827.
- (23) Sigle, D. O.; Hugall, J. T.; Ithurria, S.; Dubertret, B.; Baumberg, J. J. Probing confined phonon modes in individual CdSe nanoplatelets using surface-enhanced Raman scattering. *Physical review letters* **2014**, *113* (8), 087402.
- (24) Vong, A. F.; Irgen-Gioro, S.; Wu, Y.; Weiss, E. A. Origin of low temperature trion emission in CdSe nanoplatelets. *Nano letters* **2021**, *21* (23), 10040-10046.
- (25) Macias-Pinilla, D. F.; Planelles, J.; Climente, J. I. Biexcitons in CdSe nanoplatelets: geometry, binding energy and radiative rate. *Nanoscale* **2022**, *14* (23), 8493-8500.
- (26) Grim, J. Q.; Christodoulou, S.; Di Stasio, F.; Krahne, R.; Cingolani, R.; Manna, L.; Moreels, I. Continuous-wave biexciton lasing at room temperature using solution-processed quantum wells. *Nature nanotechnology* **2014**, *9* (11), 891-895.
- (27) Brumberg, A.; Watkins, N. E.; Diroll, B. T.; Schaller, R. D. Acceleration of Biexciton Radiative Recombination at Low Temperature in CdSe Nanoplatelets. *Nano letters* **2022**, *22* (17), 6997-7004.
- (28) Huxter, V. M.; Kovalevskij, V.; Scholes, G. D. Dynamics within the Exciton Fine Structure of Colloidal CdSe Quantum Dots. *The Journal of Physical Chemistry B* **2005**, *109* (43), 20060-20063. DOI: 10.1021/jp0546406.
- (29) Rodina, A.; Efros, A. L. Magnetic Properties of Nonmagnetic Nanostructures: Dangling Bond Magnetic Polaron in CdSe Nanocrystals. *Nano Letters* **2015**, *15* (6), 4214-4222. DOI: 10.1021/acs.nanolett.5b01566.
- (30) Rodina, A. V.; Golovatenko, A. A.; Shornikova, E. V.; Yakovlev, D. R. Spin Physics of Excitons in Colloidal Nanocrystals. *Physics of the Solid State* **2018**, *60* (8), 1537-1553. DOI: 10.1134/S106378341808019X.
- (31) Hu, R.; Wu, Z.; Zhang, Y.; Yakovlev, D. R.; Liang, P.; Qiang, G.; Guo, J.; Jia, T.; Sun, Z.; Bayer, M.; et al. Long-Lived Negative Photocharging in Colloidal CdSe Quantum Dots Revealed by Coherent Electron Spin

Precession. *The Journal of Physical Chemistry Letters* **2019**, *10* (17), 4994-4999. DOI: 10.1021/acs.jpclett.9b02341.

(32) Feng, D.; Yakovlev, D. R.; Dubertret, B.; Bayer, M. Charge separation dynamics in CdSe/CdS core/shell nanoplatelets addressed by coherent electron spin precession. *ACS nano* **2020**, *14* (6), 7237-7244.



The submitted manuscript has been created by UChicago Argonne, LLC, Operator of Argonne National Laboratory ("Argonne"). Argonne, a U.S. Department of Energy Office of Science laboratory, is operated under Contract No. DE-AC02-06CH11357. The U.S. Government retains for itself, and others acting on its behalf, a paid-up nonexclusive, irrevocable worldwide license in said article to reproduce, prepare derivative works, distribute copies to the public, and perform publicly and display publicly, by or on behalf of the Government. The Department of Energy will provide public access to these results of federally sponsored research in accordance with the DOE Public Access Plan. http://energy.gov/downloads/doe-public-access-plan